Civil, Architectural and Environmental Engineering Faculty Research & Creative Works

Civil, Architectural and Environmental Engineering

01 Oct 2010

Scale Dependence Of Radar Rainfall Uncertainty: Initial Evaluation Of NEXRAD's New Super-resolution Data For Hydrologic Applications

Bong Chul Seo
Missouri University of Science and Technology, bongchul.seo@mst.edu

Witold F. Krajewski

Recommended Citation

NOTES AND CORRESPONDENCE

Scale Dependence of Radar Rainfall Uncertainty: Initial Evaluation of NEXRAD's New Super-Resolution Data for Hydrologic Applications

BONG-CHUL SEO AND WITOLD F. KRAJEWSKI

IIHR-Hydroscience and Engineering, The University of Iowa, Iowa City, Iowa

ABSTRACT

This study explores the scale effects of radar rainfall accumulation fields generated using the new super-resolution level II radar reflectivity data acquired by the Next Generation Weather Radar (NEXRAD) network of the Weather Surveillance Radar-1988 Doppler (WSR-88D) weather radars. Eleven months (May 2008–August 2009, exclusive of winter months) of high-density rain gauge network data are used to describe the uncertainty structure of radar rainfall and rain gauge representativeness with respect to five spatial scales (0.5, 1, 2, 4, and 8 km). While both uncertainties of gauge representativeness and radar rainfall show simple scaling behavior, the uncertainty of radar rainfall is characterized by an almost 3 times greater standard error at higher temporal and spatial resolutions (15 min and 0.5 km) than at lower resolutions (1 h and 8 km). These results may have implications for error propagation through distributed hydrologic models that require high-resolution rainfall input. Another interesting result of the study is that uncertainty obtained by averaging rainfall products produced from the super-resolution reflectivity data is slightly lower at smaller scales than the uncertainty of the corresponding resolution products produced using averaged (recombined) reflectivity data.

1. Introduction

In summer of 2008, the Weather Surveillance Radar-1988 Doppler (WSR-88D) weather radars of the national Next Generation Weather Radar (NEXRAD) network began providing enhanced-resolution radar reflectivity observations. These new level II data are referred to as super resolution (Torres and Curtis 2007). While the legacy resolution of the level II data is 1° in azimuth and 1 km in range, the super-resolution data have grid spacing that is reduced to 0.5° in azimuth and to 250 m in range. However, the current algorithm used by the National Weather Service to produce nationwide radar rainfall maps (Fulton et al. 1998) does not exploit this new capability, largely because of the anticipated arrival of dual polarization (dual-polarization rain-rate products will be provided on a 250 m × 1° polar grid; Istok et al. 2009).

This resolution upgrade was motivated by the needs of severe weather detection and monitoring, and its effects have not yet been incorporated into hydrologic (rainfall) products. Although the super-resolution data may capture small-scale features of rainfall processes, NEXRAD's Precipitation Processing System (PPS) still operates based on the so-called recombined (legacy resolution) data. In this study, we explore the use of super-resolution data in rainfall estimation that is motivated by hydrologic applications. There are many physically based distributed hydrologic models that operate on grid sizes of 1 km^2 or smaller, but the readily available NEXRAD radar rainfall maps are only hourly accumulations provided on an approximately 4 × 4 km^2 grid (Fulton et al. 1998). The availability of increased resolution also offers an opportunity to systematically explore radar rainfall uncertainty over an extended range of smaller scales.

We use 11-month-long datasets from two research-grade rain gauge networks in Iowa to estimate the error variance of the super-resolution-based rainfall maps and report the results at five spatial and two temporal scales. We use the error variance separation method of Ciach and Krajewski (1999) as the main analysis tool. In section 2, we briefly describe the rain gauge and radar datasets used and the error variance estimation methodology. In section 3, we provide the results and discuss

Corresponding author address: Witold F. Krajewski, IIHR-Hydroscience and Engineering, The University of Iowa, Iowa City, IA 52242.
E-mail: witold-krajewski@uiowa.edu

them in the context of earlier studies of radar rainfall uncertainty (Ciach et al. 2007). Lastly, section 4 concludes and summarizes our study's main findings and limitations.

2. Data and methodology

Our research group operates two high-quality, high-density rain gauge networks in Iowa. The larger network, centered on the Iowa City Municipal Airport (Fig. 1), comprises more than 30 sites. Last year, only 19 sites were operational. The network is located between 80 and 120 km from the Davenport, Iowa, WSR-88D (KDVN). At each site, there are two tipping-bucket gauges, a datalogger, and a cell phone, all powered by a battery that is charged by a solar panel (Fig. 1). The average intergauge spacing of the network is about 5 km. Time-of-tip data (see Ciach 2003) are recorded on-site and transmitted to a database server every 15 min. This automatic process performs data quality control by comparing data from the two rain gauges and makes rainfall products (accumulations) at multiple time scales from 5 min to daily. These rainfall products are stored in a relational database and made available to researchers over the Internet using a browser-based interface.

The second network is located just south of Ames, Iowa, in support of a National Aeronautics and Space Administration (NASA)-funded study of remote sensing of soil moisture. That network is a cluster of seven sites (Fig. 1) that are equipped identically to the Iowa City network. The cluster is about 30 km north of the Des Moines, Iowa, WSR-88D (KDMX). Both networks collect rainfall data only and are not deployed during the winter months.

For our radar datasets, we used the super-resolution level II reflectivity data of the KDMX and KDVN radars. The radars have started collecting reflectivity data in super resolution from May and June 2008, respectively. The data included in our study extend from the dates the radars switched to the new mode through August 2009, thus including the rainfall events that led to extreme flooding in eastern Iowa but excluding winter months from November 2008 through March 2009.

Since the PPS does not support super-resolution data, we used another community-based algorithm to study the scale effect of radar rainfall uncertainty. To convert the reflectivity data to rainfall accumulation maps, we used the Hydro-NEXRAD system developed to support hydrologic research (Vasiloff et al. 2007; Krajewski et al. 2010; Kruger et al. 2010; Seo et al. 2010). We modified the Hydro-NEXRAD algorithms for the new super-resolution data processing and used them offline (i.e.,

super-resolution-based products are currently not available via Hydro-NEXRAD). The algorithms process super-resolution reflectivity data and produce rainfall accumulations using the NEXRAD reflectivity-to-rainfall-rate (Z–R) relationship ($Z = 300R^{1.4}$; see Fulton et al. 1998) at 15-min and 1-h scales on fixed polar grid spacing (0.5° in azimuth and 250 m in range). The polar grid products are then transformed to various spatial scales using the Hydrologic Rainfall Analysis Project (HRAP) grid projection (Reed and Maidment 1999) with spacing of approximately 0.5-, 1-, 2-, 4-, and 8-km grids. We then applied the nearest neighbor and weighted-averaging grid transformation (interpolation) schemes and attempted to mimic the recombination algorithm that transforms super-resolution reflectivity data into legacy resolution before feeding such data into the Hydro-NEXRAD rainfall algorithms. This is to show how the averaging in the volume scan data affects the uncertainty of the final products.

To assess the super-resolution products, we performed a rain gauge comparison with the super-resolution rainfall estimates as well as with other products, that is, recombined digital precipitation array (DPA) provided by the National Oceanic and Atmospheric Administration (NOAA)'s National Climatic Data Center (NCDC) and commonly used by hydrologic users. The grid system of the DPA radar-rainfall products is the 4×4 km^2 HRAP. To compare the DPA with the super-resolution products averaged to the HRAP scale, we used the corresponding rain gauge data for gauges located in the respective HRAP grid.

The time span of this hourly comparison is also from the commencement of super resolution through the end of August 2009. As described in Table 1, the statistical properties of the radar rainfall products were characterized by the correlation coefficient, the multiplicative bias, and the root-mean-square error (RMSE). On the basis of these three statistics, the scatterplots of Fig. 2, and the two-sample t test (Moore 2003), the super resolution tends to be consistent with the DPA. The null hypothesis for the test (two sided) is that the mean differences between both radar rainfall and rain gauge rainfall are the same. The p value (0.18) demonstrates that both products are statistically consistent with a 95% confidence interval. However, statistics values in Table 1 show little difference (especially bias), which may be caused by the discrepancy of polar grids between super resolution and legacy resolution or that of rainfall algorithms, that is, the hybrid scan structure at near range from the radar between PPS and Hydro-NEXRAD [for more detail, see Fulton et al. (1998); Seo et al. (2010)]. Overall, the hourly comparison results illustrate that the super-resolution estimates computed by the Hydro-NEXRAD
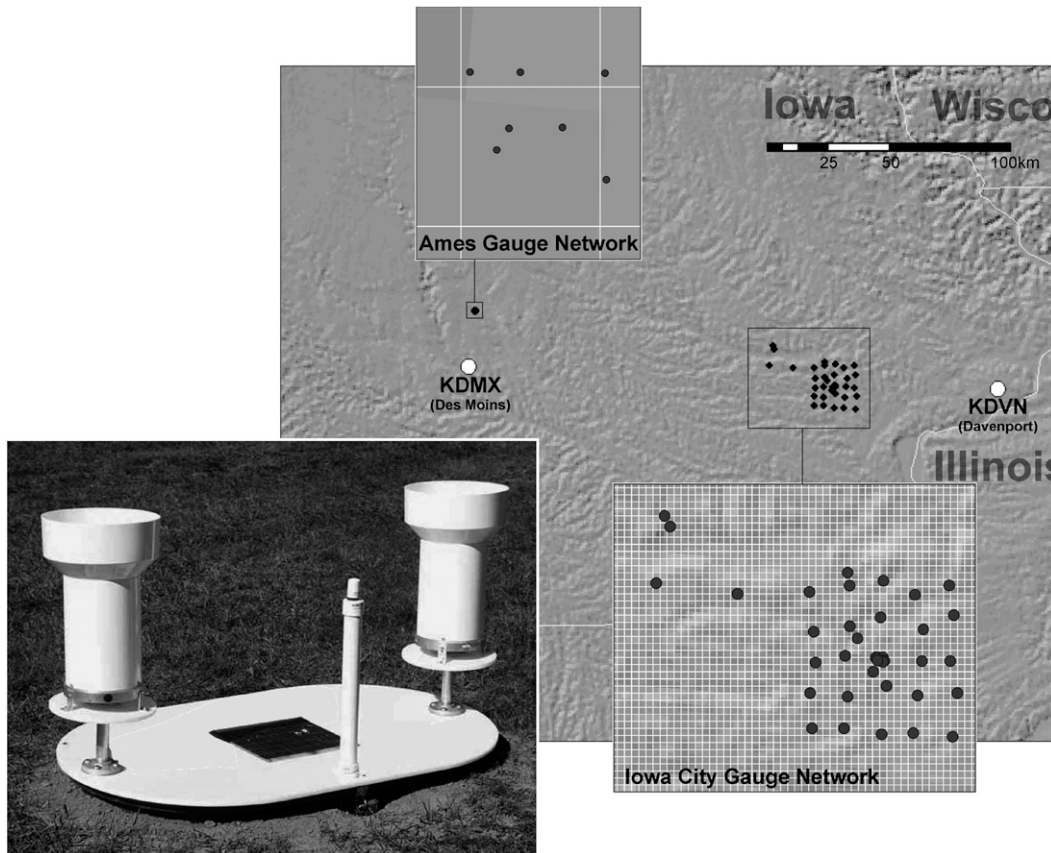
FIG. 1. Two rain gauge networks used in Iowa and the structure of tipping-bucket gauges. The grid cells seen in both networks represent 1-km spacing.

algorithm are compatible with the DPA, which gives credence to the remaining part of this study.

The error variance separation method (Ciach and Krajewski 1999) requires the use of the spatial correlation function of rainfall at the appropriate temporal scale—in our case, at the 15-min and hourly scales. The spatial correlation function describes the spatial dependence of rainfall processes, which significantly affects the variance reduction (Morrissey et al. 1995) of point-to-area estimation error. Its estimation is difficult because of the bias that arises from the high skewness of rainfall variables. Because of the bias problem of the traditional estimator—that is, Pearson's product-moment correlation coefficient (see, e.g., Stedinger 1981)—Habib et al. (2001) proposed a transformation procedure for log-normally distributed rainfall data. In addition, the sample correlation might be considerably affected by abnormal values beyond the overall pattern of a sample distribution (e.g., outliers); thus, the use of another estimator to represent spatial processes, a variogram (or semivariogram), is usually preferred (Cressie 1993). We did not apply the procedure of Habib et al. (2001)

since the empirical distribution of the rainfall data showed no significant thick tail in the range of extreme rainfall values, implying that our rainfall data are not log-normally distributed (see also Ciach and Krajewski 2006). Thus, we estimated the spatial correlation structure of rain fields using a covariance function derived from the variogram (Schabenberger and Gotway 2005), assuming the intrinsic hypothesis and second-order stationary process. Because

TABLE 1. Values of statistics for hourly gauge data comparison with super-resolution and DPA estimates based on the HRAP scale. The statistics values were computed using 14 radar–gauge pairs for KDVN-Iowa City network and only 1 radar-gauge pair for KDMX-Ames network. The gauge mean and standard deviation values are 0.18 and 1.26 for Iowa City network and 0.16 and 1.19 for Ames network.

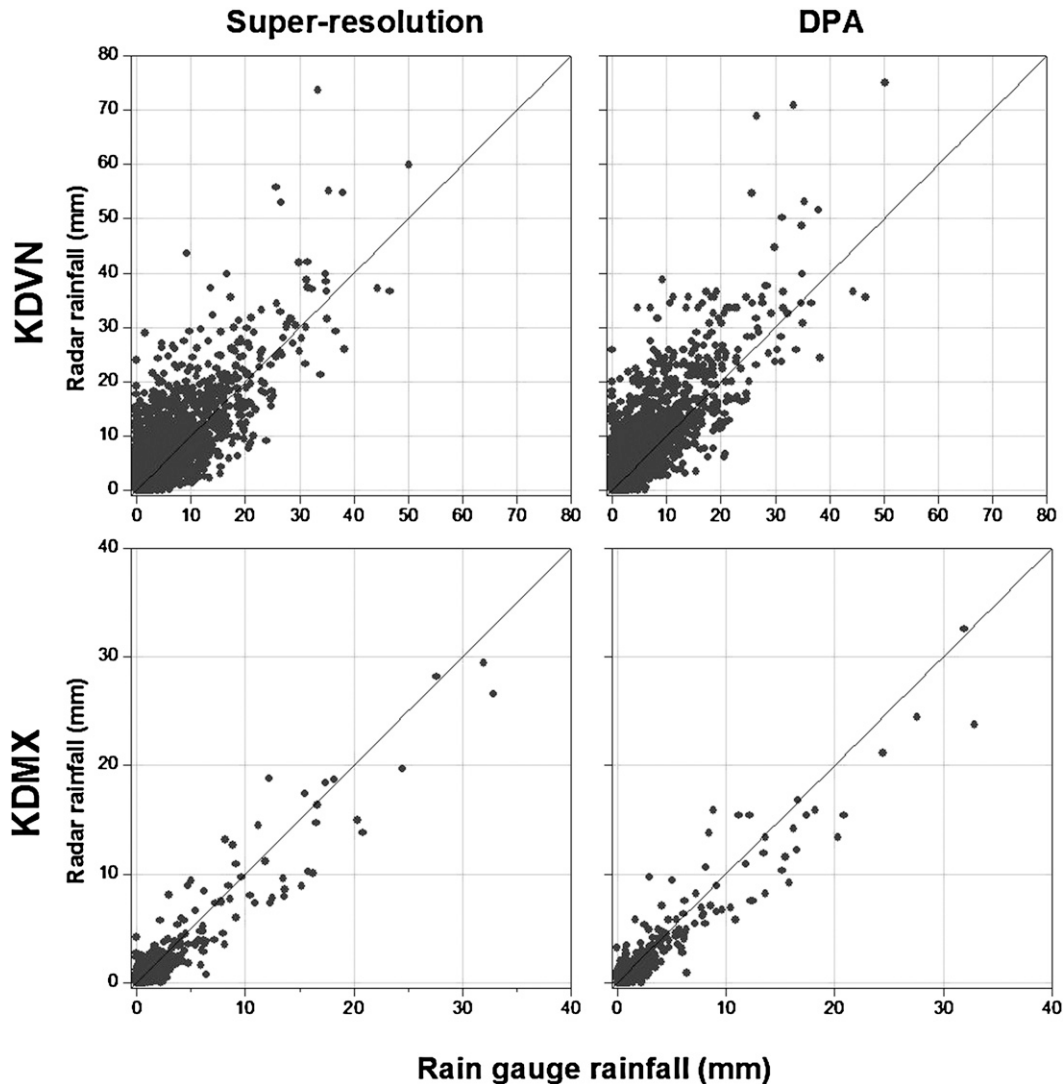| Statistics	KDVN-Iowa City network		KDMX-Ames network	
	Super resolution	DPA	Super resolution	DPA
Correlation	0.87	0.88	0.95	0.96
Bias	0.78	0.67	1.20	1.07
RMSE	0.64	0.61	0.39	0.37

FIG. 2. Scatterplots of hourly gauge comparison with (left) super-resolution and (right) DPA estimates for (top) KDVN-Iowa City network and (bottom) KDMX-Ames network radar–gauge pairs. For rain gauges within the same HRAP grid, involved rain gauge data were averaged.

our smaller rain gauge network cannot provide the necessary correlation information for the scales (i.e., 2, 4, and 8 km) larger than its domain, a three-parameter exponential function represented by nugget, correlation distance, and shape factors [for more information on these parameters, see Journel and Huijbregts (1978); Krajewski et al. (2000)] was estimated using the larger network some 150 km due east in Iowa City.

On the other hand, we use rain gauge data from the smaller network and radar rainfall estimates from the KDMX radar for the error variance analysis. Using this pair of radar–gauge data can prevent one of the significant radar rainfall error sources—namely, the range-dependent error—reported by Smith et al. (1996). Since anomalous propagation (AP) might be a major error

source in the warm and cold seasons at near range around the radar, we also removed it using an adaptation of the algorithm by Steiner and Smith (2002).

Given the spatial correlation structure and radar–gauge differences, the error variances are separated based on (i) two temporal (15 min and hourly) and five spatial (0.5, 1, 2, 4, and 8 km) scales, (ii) super resolution and recombination to legacy resolution, and (iii) the nearest neighbor and the averaging schemes for the spatial transformation of rainfall fields.

3. Results

In this section, we present the results related to the spatial correlation functions and the uncertainty structure

TABLE 2. Relative error standard deviation (mm mm^{-1}) normalized by the mean value of ground measurements with respect to scale.

| Temporal scale | Spatial scale (km) | Radar rainfall | | | | Rain gauge representativeness |
| | | Super resolution | | Recombination | | |
		Nearest	Averaging	Nearest	Averaging	
15 min	0.5	1.78	1.70	—	—	0.24
	1.0	1.75	1.59	1.71	1.60	0.36
	2.0	1.66	1.45	1.61	1.44	0.44
	4.0	1.41	1.00	1.40	0.99	0.65
	8.0	1.37	0.63	1.31	0.56	1.07
1 h	0.5	1.16	1.13	—	—	0.12
	1.0	1.14	1.06	1.12	1.07	0.18
	2.0	1.09	0.98	1.07	1.00	0.23
	4.0	0.91	0.71	0.91	0.70	0.35
	8.0	0.91	0.52	0.88	0.48	0.61

of gauge representativeness and super-resolution rainfall estimates with respect to scale.

For respective temporal accumulation scales (15 min and hourly), spatial correlation functions are characterized by the nugget effect (0.97 and 1.00), correlation distance (21 and 36 km), and the shape factor (1.05 and 1.11). While hourly data show relatively stronger spatial dependence based on all three parameters, as expected, 15-min data represent higher variability of the spatial process. This implies that a longer time span of data integration reduces the spatial variability of the rainfall process. In addition, spatial dependence described by the aforementioned correlation distances seems stronger than in other areas [Florida (Habib et al. 2001) and Oklahoma (Ciach and Krajewski 2006)] in the United States where hurricane and more convective systems are major sources of the rainfall process. To compute the variance reduction of point-to-area estimation error, the distance range of interest in the estimated functions is about 11 km, considering the largest grid of 8 km.

Table 2 presents the error variance with respect to scale, represented by relative error standard deviation that is normalized by the mean of the rain gauge measurements. No rain events, determined based on rain gauge observations, were excluded from the analysis. Also, the 0.5-km rainfall maps for recombined data were not produced because of the larger grid spacing of legacy resolution. Overall, both rain gauge representativeness error and radar rainfall error seem to change systematically with respect to spatial scale. As grid spacing is smaller, the uncertainty of gauge representativeness decreases and that of radar rainfall increases. Also, a shorter sampling scale over time results in higher uncertainties at all spatial scales. In terms of the spatial transformation, the averaging shows lower variance at all scales. This property tends to be more significant at shorter time and larger spatial scales (i.e., 15 min and 8 km), where more polar pixel values are averaged over

a corresponding projected grid. However, improvement due to the use of an averaging scheme over a computationally faster nearest neighbor scheme seems to matter little at the smallest scale (i.e., 3% reduction at 0.5-km and 1-h scales). For the comparison between super resolution and recombination, the uncertainty of super resolution is slightly lower at smaller scales (1 and 2 km).

Figure 3 clearly illustrates the structure of both uncertainties for the averaging scheme. Both uncertainties show an interesting aspect of scaling behavior with respect to spatial scale. Linear behavior in log-log units implies power-law dependence on scale. In addition, the super-resolution estimates at the smallest scale (0.5 km) are approximately 3 times (at the 15-min scale) and 2 times (at the hourly scale) more uncertain than at the largest scale (8 km). These uncertainty differences between scales may have implications for error propagation through distributed hydrologic models that require high-resolution rainfall input. Considering the most common hydrologic radar rainfall resolution (4 km and hourly accumulations), the super-resolution estimates are characterized by 70% uncertainty of the hourly mean value of rainfall.

In addition to the analysis of additive error presented earlier, we also quantify the super-resolution uncertainty represented by multiplicative errors conditioned on rainfall magnitude (at 4-km and hourly scale) similarly to Ciach et al. (2007). For this analysis, we used the hourly 4-km products derived from super-resolution data and assumed no "deterministic distortion" (see Ciach et al. 2007) for our data because the rain gauge locations for the Ames network are sufficiently close to the radar (implying that the distortion should not be significant), and it is hard to estimate the distortion function with the relatively small sample size of our data. The uncertainty described by conditional error standard deviation for the warm (April, May, and October) and hot (June–September) seasons is presented in Fig. 4. The functional structure of super-resolution uncertainty is
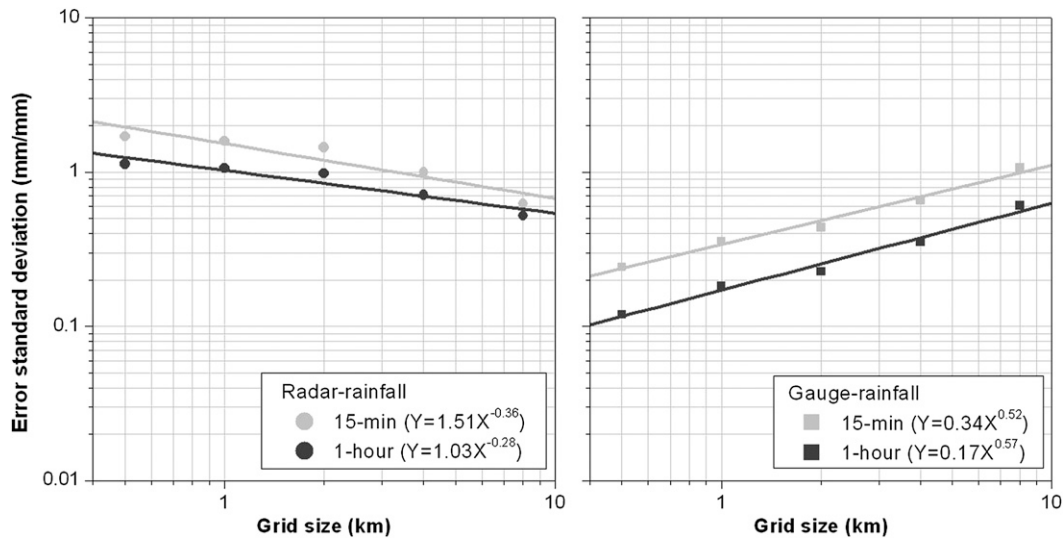
FIG. 3. Relative error standard deviation (normalized by the mean of rain gauge measurements) of super-resolution estimates and gauge representativeness with respect to spatial scale.

similar to that reported by Ciach et al. (2007), but super resolution shows lower radar rainfall uncertainty. The lower uncertainty could either be due to using super resolution or our smaller sample size [1 yr versus 6 yr used by Ciach et al. (2007)] and/or sampling locations closer to the radar in this study.

4. Conclusions and discussion

We report scale effects for the uncertainties of the radar rainfall estimates obtained using the new super-resolution data from the NEXRAD radars. Since the super-resolution-based rainfall maps are not operationally available from federal agencies, this early effort provides unique information on the potential advantages of the new data. Our findings are summarized as follows.

1) The hourly comparison between the super resolution and the DPA data demonstrates statistical consistency.

2) Super resolution shows slightly lower uncertainty at smaller scales. This indicates that using super-resolution data for hydrologic applications that require
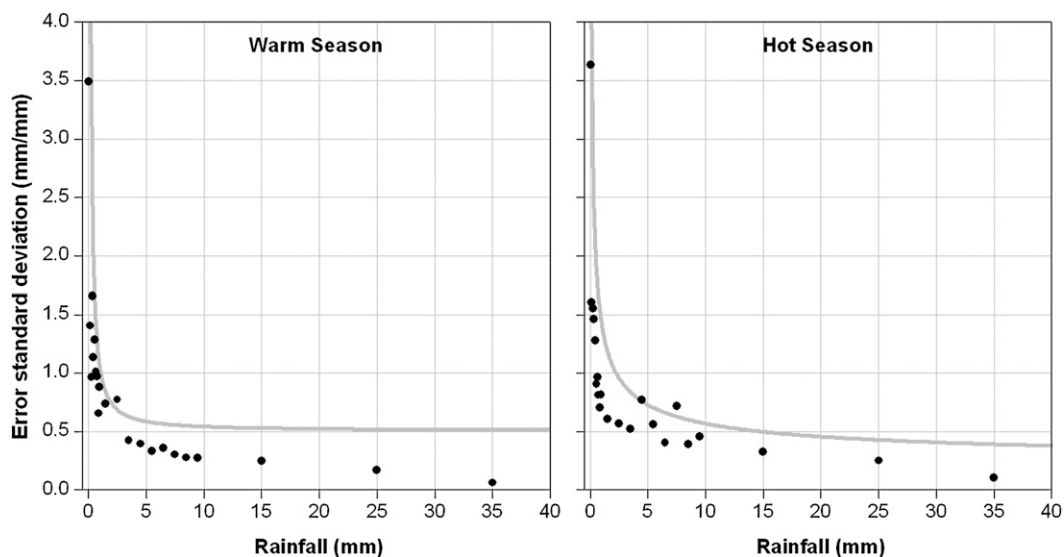

FIG. 4. Multiplicative error standard deviation conditioned on rainfall magnitude empirically estimated from 4-km and hourly super-resolution estimates. Solid lines were presented from Table 4 of Ciach et al. (2007).

higher-resolution input may mitigate the uncertainty of rainfall input. However, it is likely that the improvement is relatively small for the magnitude of uncertainty itself.

3) Using the averaging scheme for spatial grid transformation reduces radar rainfall uncertainty regardless of scale. As the scale becomes larger, the uncertainty decreases more significantly. However, the nearest neighbor scheme may be an alternative to higher-resolution data since uncertainty differences between the two schemes severely decrease as the spatial scale becomes smaller.

4) There is a systematic uncertainty behavior of the radar rainfall and the gauge representativeness with respect to scale. They all show a simple scaling law. The radar rainfall uncertainty is characterized by an almost 3 times greater standard error at higher resolutions (15 min and 0.5 km) than at lower resolutions (1 h and 8 km). This result may imply that the error of radar rainfall propagates through distributed hydrologic models that require high-resolution rainfall input.

Since super-resolution data have only been collected in the past year, the results and conclusions are valid for this limited period of data. In the future, extending datasets will be necessary to comprehensively evaluate super-resolution data and to fully understand the benefit of using super-resolution data and the statistical structure of the uncertainty. In addition, addressing the uncertainty of spatial correlation estimation and its propagation to the variance reduction for point-to-area estimation error may enhance comprehension of the uncertainty structure of involved rainfall data. Lastly, in the present study we ignored the possibility of radar and rain gauge error being correlated (see, e.g., Ciach and Krajewski 1999; Ciach et al. 2003); however, in the absence of well-documented evidence to the contrary, this seems justifiable in this preliminary study.

REFERENCES

Ciach, G. J., 2003: Local random errors in tipping-bucket rain gauge measurements. *J. Atmos. Oceanic Technol.,* **20,** 752–759.

——, and W. F. Krajewski, 1999: On the estimation of radar rainfall error variance. *Adv. Water Resour.,* **22,** 585–595.

——, and ——, 2006: Analysis and modeling of spatial correlation structure of small-scale rainfall in Central Oklahoma. *Adv. Water Resour.,* **29,** 1450–1463.

——, E. Habib, and W. F. Krajewski, 2003: Zero-covariance hypothesis in the Error Variance Separation method of radar rainfall verification. *Adv. Water Resour.,* **26,** 673–680.

——, W. F. Krajewski, and G. Villarini, 2007: Product-error-driven uncertainty model for probabilistic quantitative precipitation estimation with NEXRAD data. *J. Hydrometeor.,* **8,** 1325–1347.

Cressie, N. A. C., 1993: *Statistics for Spatial Data.* John Wiley and Sons, 900 pp.

Fulton, R. A., J. P. Breidenbach, D.-J. Seo, D. A. Miller, and T. O'Bannon, 1998: The WSR-88D rainfall algorithm. *Wea. Forecasting,* **13,** 377–395.

Habib, E., W. F. Krajewski, and G. J. Ciach, 2001: Estimation of rainfall interstation correlation. *J. Hydrometeor.,* **2,** 621–629.

Istok, M., and Coauthors, 2009: WSR-88D dual polarization initial operational capabilities. Preprints, *25th Conf. on International Interactive Information and Processing Systems (IIPS) for Meteorology, Oceanography, and Hydrology,* Phoenix, AZ, Amer. Meteor. Soc., 15.5. [Available online at http://ams.confex.com/ams/pdfpapers/148927.pdf.]

Journel, A. G., and Ch. J. Huijbregts, 1978: *Mining Geostatistics.* Academic Press, 600 pp.

Krajewski, W. F., G. J. Ciach, J. R. McCollum, and C. Bacotiu, 2000: Initial validation of the Global Precipitatioin Climatology Project over the United States. *J. Appl. Meteor.,* **39,** 1071–1086.

——, and Coauthors, 2010: Towards better utilization of NEXRAD data in hydrology: An overview of Hydro-NEXRAD. *J. Hydroinf.,* doi:10.2166/hydro.2010.056, in press.

Kruger, A., W. F. Krajewski, and P. Domaszczynski, 2010: Hydro-NEXRAD: Metadata computation and use. *J. Hydroinf.,* doi:10.2166/hydro.2010.057, in press.

Moore, S. D., 2003: *The Basic Practice of Statistics.* 3rd ed. W. H. Freeman and Company, 440–444 pp.

Morrissey, M. L., J. A. Maliekal, J. S. Greene, and J. Wang, 1995: The uncertainty of simple spatial averages using rain gauge networks. *Water Resour. Res.,* **31,** 2011–2017.

Reed, S. M., and D. R. Maidment, 1999: Coordinate transformations for using NEXRAD data in GIS-based hydrologic modeling. *J. Hydrol. Eng.,* **4,** 174–182.

Schabenberger, O., and C. A. Gotway, 2005: *Statistical Methods for Spatial Data Analysis.* Statistical Science Series, Chapman & Hall/CRC, 488 pp.

Seo, B.-C., W. F. Krajewski, A. Kruger, P. Domaszczynski, J. A. Smith, and M. Steiner, 2010: Radar-rainfall estimation algorithms of Hydro-NEXRAD. *J. Hydroinf.,* in press.

Smith, J. A., D.-J. Seo, M. L. Baeck, and M. D. Hudlow, 1996: An intercomparison study of NEXRAD precipitation estimates. *Water Resour. Res.,* **32,** 2035–2045.

Stedinger, J. R., 1981: Estimating correlations in multivariate streamflow models. *Water Resour. Res.,* **17,** 200–208.

Steiner, M., and J. A. Smith, 2002: Use of three-dimensional reflectivity structure for automated detection and removal of nonprecipitating echoes in radar data. *J. Atmos. Oceanic Technol.,* **19,** 673–686.

Torres, S. M., and C. D. Curtis, 2007: Initial implementation of super-resolution data on the NEXRAD network. Preprints, *23rd Conf. on International Interactive Information and Processing Systems (IIPS) for Meteorology, Oceanography, and Hydrology,* San Antonio, TX, Amer. Meteor. Soc., 5B.10. [Available online at http://ams.confex.com/ams/87ANNUAL/techprogram/paper_116240.htm.]

Vasiloff, S. V., and Coauthors, 2007: Improving QPE and very short-term QPF: An initiative for a community-wide integrated approach. *Bull. Amer. Meteor. Soc.,* **88,** 1899–1911.